Nature of Prominences and their role in Space Weather
Proceedings IAU Symposium No. 300, 2013
B. Schmieder, J.-M. Malherbe & S. T. Wu, eds.

doi:10.1017/S1743921313011071

Flux rope axis geometry of magnetic clouds deduced from in situ data

Miho Janvier[1], Pascal Démoulin[1] and Sergio Dasso[2]

[1]Observatoire de Paris, LESIA, UMR 8109 (CNRS), F-92195 Meudon Principal Cedex, France
email: miho.janvier@obspm.fr, pascal.demoulin@obspm.fr

[2]Departamento de Física e Instituto de Astronomía y Física del Espacio (UBA-CONICET), Facultad de Ciencias Exactas y Naturales, Universidad de Buenos Aires, 1428 Buenos Aires, Argentina
email: dasso@df.uba.ar

Abstract. Magnetic clouds (MCs) consist of flux ropes that are ejected from the low solar corona during eruptive flares. Following their ejection, they propagate in the interplanetary medium where they can be detected by in situ instruments and heliospheric imagers onboard spacecraft. Although in situ measurements give a wide range of data, these only depict the nature of the MC along the unidirectional trajectory crossing of a spacecraft. As such, direct 3D measurements of MC characteristics are impossible. From a statistical analysis of a wide range of MCs detected at 1 AU by the *Wind* spacecraft, we propose different methods to deduce the most probable magnetic cloud axis shape. These methods include the comparison of synthetic distributions with observed distributions of the axis orientation, as well as the direct integration of observed probability distribution to deduce the global MC axis shape. The overall shape given by those two methods is then compared with 2D heliospheric images of a propagating MC and we find similar geometrical features.

Keywords. Sun: coronal mass ejections (CMEs), Sun: magnetic fields, interplanetary medium

1. Introduction

Magnetic clouds (MCs) form a subclass of Interplanetary Coronal Mass Ejections (ICMEs), which are released in the interplanetary medium during eruptive flares (Gosling *et al.* 1990). As they transport a large amount of plasma material and magnetic flux, they are amongst the main drivers of space weather (Gosling 1993; Marubashi 2000). Although an ICME definition depends on measurements and authors (see review of Démoulin 2014), MCs are strictly defined, for example, by an enhanced magnetic field strength and a smooth rotation of the magnetic field direction through a large angle (Dasso *et al.* 2005). This magnetic field rotation indicates the existence of a flux rope (FR) (e.g., Lepping *et al.* 1990; Dasso *et al.* 2006) that is well correlated with observations of eruptive flare configurations (e.g., Zhang *et al.* 2012; Title 2014), as well as with theoretical models reproducing the underlying processes of eruptive flares (e.g., the tether cutting model of Moore *et al.* 1997 or the torus-unstable model of Aulanier *et al.* 2010).

Understanding the structure of MCs is important for several reasons. For example, knowing the characteristics of the magnetic FR can help us to understand the role of the field line length in the time delay of energetic particles detection (see Larson *et al.* 1997 and Masson *et al.* 2012). Similarly, it can help us to link MC structures with the 3D configuration of the associated solar source (see Nakwacki *et al.* 2011), as well as to calculate the budget for the magnetic helicity, magnetic energy and flux (e.g., Dasso *et al.* 2005 and Démoulin *et al.* 2002).

However, deriving the 3D MC structure is not at all straightforward from one sample of data; as the spacecraft is crossing the MC along a unidirectional trajectory, it can

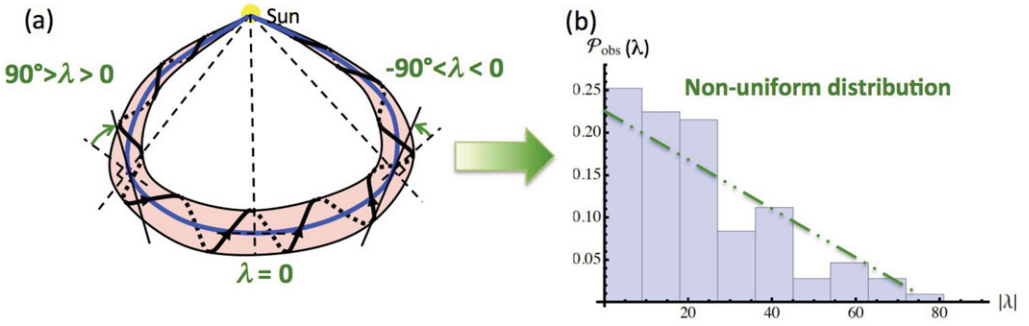

Figure 1. (a) Definition of the location angle, λ, and (b) the related non-uniform distribution from observations of a set of 107 MCs observed by *Wind*.

only locally measure MC characteristics. Then, from 1D data, several different fitting procedures can be applied (see review of Démoulin 2014) but all of them necessitate more or less drastic hypotheses (e.g., Sonnerup *et al.* 2006). All in all, information of one event extrapolated from 1D measured parameters to get the 3D characteristics of a MC can lead to a large error when estimating its properties.

One solution to this problem is to have multiple spacecraft crossings (e.g., Kilpua *et al.* 2011). However, the occurence of such an event is too rare to properly investigate the general characteristics of MCs. In the following, we propose a new study based on statistical analyses of a sample of several MCs crossed by the same spacecraft and fitted by the same analytical model. In particular, we are interested in the most probable shape of the FR axis of observed MCs. The methodology, results and discussion are summarized in the present paper, but more information are found in Janvier *et al.* (2013).

2. Location angle, λ, distribution

In the present work, MCs properties are investigated via a statistical analysis of MC measurements so as to deduce the general FR axis shape. The set of MCs that is chosen is a sample of 107 MCs detected by the *Wind* spacecraft (located at 1 AU) during 15 years (Lepping & Wu 2010). This list also gives their physical characteristics following the Lundquist fitting model (see Lundquist 1950), such as their sizes and their orientations. In addition, we introduce two new orientation angles, namely the inclination angle, i, which measures the angle between the plane of the MC axis and the ecliptic plane, and the location angle, λ, that measures the angle between the local direction of the MC axis and the orthoradial (see Fig. 1a, where λ can be understood as the location of the spacecraft regarding the MC). These two parameters are more adapted to the study of the FR axis shape than the standard direction parameters (longitude and latitude).

From the list of MC parameters, a problem can be raised: since all MCs have different characteristics (in terms of speed, size, ...), can a sample of MCs be considered as a whole so as to statistically analyze the behavior of one parameter? Would it not be necessary to categorize MCs in sub-classes so as to properly investigate this parameter? In other words, if the FR axis shape is analyzed via the location angle λ, does not this shape also depend on other intrinsic properties of MCs?

To answer this question, the distribution of the location angle, λ, (Fig.1b) was thoroughly investigated as a function of all the other MCs parameters. Especially, sub-groups of MCs ordered in function of their characteristics (say, the radius) were made, so as to investigate the changes in the λ-distribution. Since no changes can be reported, and as

https://doi.org/10.1017/S1743921313011071 Published online by Cambridge University Press

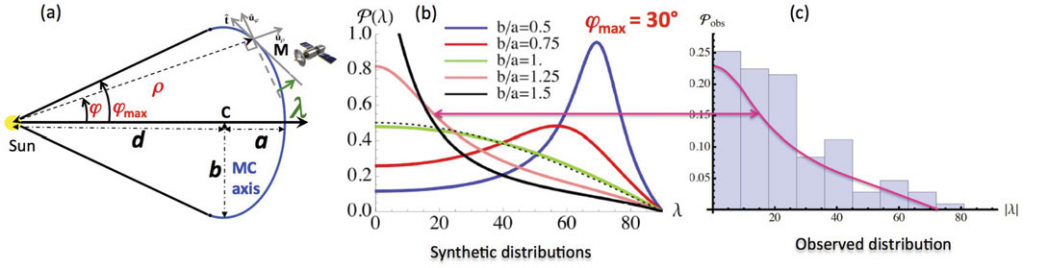

Figure 2. (a) Diagram representing the analytical ellipse shape given to the FR axis, with parameters ρ and φ in cylindrical coordinates. **(b)** Synthetic distributions deduced from the analytical shapes when varying the aspect ratio, at fixed $\varphi_{\max} = 30°$. **(c)** Matching of the synthetic distribution for aspect ratio = 1.25 with the observed probability distribution.

there is only a very weak correlation between λ and all other MCs intrinsic parameters, we verified that the *Wind* sample of 107 MCs can be analyzed together as a whole, so as to deduce the most probable axis shape from this set of data.

Let us now focus on the properties of the λ distribution function. Contrary to the distribution of the inclination angle, i, which is flat (see Janvier *et al.* 2013), the distribution of the location angle is non-uniform. A flat distribution for i implies that there is no privileged inclination for the detection of a MC by a spacecraft: North/South or East/West MCs are detected the same. However, a non-uniform decreasing distribution of $|\lambda|$, $\mathcal{P}_{\rm obs}(\lambda)$, implies that MCs are more often detected at the apex (see Fig. 1a) than in the legs. This is an interesting property that has implications on the axis shape of the FR.

To investigate the characteristics of $\mathcal{P}_{\rm obs}(\lambda)$, we propose two joint methods. First, synthetic distributions are derived from an analytical MC model, and are then compared with $\mathcal{P}_{\rm obs}(\lambda)$. As a second step, $\mathcal{P}_{\rm obs}(\lambda)$ is directly integrated so as to derive the most probable FR axis shape.

3. Flux rope axis shape deduced from two statistical methods

Synthetic distributions method. This first method implies creating synthetic distributions from an analytical model of a FR axis shape and comparing them with $\mathcal{P}_{\rm obs}(\lambda)$. We analyze the shape of the FR axis as an ellipse joined at two ends to the Sun. The ellipse is parametrized in cylindrical coordinates by the radius, ρ, and the rotation angle, φ, that are themselves expressed as a function of the ellipse parameters (Fig.2a). The full extension of the ellipse is given as $\varphi_{\max}$. From this analytical shape, we can derive an expression of a probability distribution for λ: $\mathcal{P}_{\rm synth}(\lambda) = \mathcal{P}(\varphi)|d\varphi/d\lambda|$ where $\mathcal{P}(\varphi) = 1/(2\varphi_{\max})$. Different $\mathcal{P}_{\rm synth}(\lambda)$ are obtained by varying the axis shape. Then, when compared with the observed probability distribution (Fig.2c), we found a very good correlation for an aspect ratio of the ellipse, $b/a = 1.25$. Note that those results depend on one free parameter, $\varphi_{\max}$. However, by changing its values, we checked that $\varphi_{\max}$ has a small effect on the shapes taken by $\mathcal{P}_{\rm synth}(\lambda)$ contrary to the aspect ratio.

Direct derivation of the FR axis shape from $\mathcal{P}_{\rm obs}(\lambda)$. As a second method, we directly use the observed distribution. By integrating $\mathcal{P}_{\rm obs}(\lambda)$, we express the parameters ρ and φ of the FR axis shape in cylindrical coordinates (without assuming any preconceived ellipse shape). Note here that, similarly with the first method, there is one free parameter, $\varphi_{\max}$, that cannot be constrained. As such, different shapes are derived, depending on

https://doi.org/10.1017/S1743921313011071 Published online by Cambridge University Press

the values of the maximum elongation, but all are similar to that found with the first method, making both methods consistent.

Comparison with heliospheric imagers. Since heliospheric imagers give information on the shape of propagating structures from the Sun, we use such data to compare the FR axis shapes seen in 2D images with that found by statistical methods. For that, we chose an event that was best seen in terms of FR detection. This event was recorded by HI imagers onboard STEREO-A (see Möstl *et al.* 2009). We then repeated several times manual pointing of the FR axis in different images, and tracked its propagation. We found that although the FR grows larger with time, there is a self-similarity in the shape of the axis that can be directly compared with the shapes obtained with the previous methods. Furthermore, using the heliospheric images allowed us to constrain the free parameter, $\varphi_{\max}$, to 30°.

4. Conclusion

The present paper summarizes different methods used to derive the most probable FR axis shape. For that, we used in situ data from a sample of MCs detected by *Wind* spacecraft over 15 years. In particular, we studied the characteristics of the non-uniform distribution of the location angle, λ, a parameter that is directly related to the location of the spacecraft along the FR axis, and therefore to its shape. After verifying that λ was strictly uncorrelated with all other MC parameters, to ensure the consistency of the full set of data, we compared synthetic distributions obtained from analytical FR axis shape with the observed distribution. Similar results with this method and with the direction integration of the observed distribution were found. Then, for completeness of the study, we finally used heliospheric images to compare the shape observed in a propagating MC with shapes determined with in situ data. All those methods prove to be consistent and we were able to find the most probable shape of FR axis (see Figs 10 and 12 in Janvier *et al.* 2013).

References

Aulanier, G., Török, T., Démoulin, P., & DeLuca, E. E. 2010, *Astrophysical Journal*, 708, 314
Dasso, S., Mandrini, C. H., Démoulin, *et al.* 2005, *Adv. Spa. Res.*, 35, 711
Dasso, S., Mandrini, C. H., Démoulin, P., & Luoni, M. L. 2006, *A&A*, 455, 349
Démoulin, P., Mandrini, C. H., van Driel-Gesztelyi, L., *et al.* 2002, *A&A*, 382, 650
Démoulin, P. 2014, *Solar Physics*, this issue
Gosling, J. T., Bame, S. J., McComas, D. J., & Phillips, J. L. 1990, *Geo. Res. Let.*, 17, 901
Gosling, J. T. 1993, *Physics of Fluids B*, 5, 2638
Janvier, M., Démoulin, P., & Dasso, S. 2013, *A&A*, 556, A50
Kilpua, E. K. J., Jian, L. K., Li, *et al.* 2011, *Jour. Atmos. Sol.-Ter. Phys.*, 73, 1228
Larson, D. E., Lin, R. P., McTiernan, J. M. *et al.* 1997, *Geophysical Research Letters*, 24, 1911
Lepping, R. P., Burlaga, L. F., & Jones, J. A. 1990, *J. Geophys. Res.*, 95, 11957
Lepping, R. P. & Wu, C. C. 2010, *Ann. Geophys.*, 28, 1539
Lundquist, S. 1950, *Ark. Fys.*, 2, 361
Marubashi, K. 2000, *Adv. Spa. Res.*, 26, 55
Masson, S., Démoulin, P., Dasso, S., & Klein, K.-L. 2012, *A&A*,, 538, A32
Moore, R. L., Schmieder, B., Hathaway, D. H., & Tarbel, T. D. 1997, *Solar Physics*, 176, 153
Möstl, C., Farrugia, C. J., Temmer, M., *et al.* 2009, *Astrophysical Journal*, 705, L180
Nakwacki, M., Dasso, S., & Démoulin, P. 2011, *A&A*,, 535, A52
Sonnerup, B. U., Hasegawa, H., Teh, W.-L., & Hau, L.-N. 2006, *Jour. Geophys. Res.*, 111, A09204
Title, A. 2014, *Solar Physics*, this issue
Zhang, J., Cheng, X., & Ding, M. 2012, *Nature communications*, 3, 747

https://doi.org/10.1017/S1743921313011071 Published online by Cambridge University Press